Inorg. Chem. **2007**, *46*, 7923–7934

Lanthanide Complexes of the Chiral Hexaaza Macrocycle and Its *meso*-Type Isomer: Solvent-Controlled Helicity Inversion

Janusz Gregoliński, Katarzyna Ślepokura, and Jerzy Lisowski*

Department of Chemistry, University of Wrocław, 14 F. Joliot-Curie, 50-383 Wrocław, Poland

Received April 30, 2007

Lanthanide(III) complexes of the enantiopure chiral hexaaza tetraamine macrocycle L, 2(*R*),7(*R*),18(*R*),23(*R*)-1,8,-15,17,24,31-hexaazatricyclo[25.3.1.1.0.0]-dotriaconta-10,12,14,26,28,30-hexaene, as well as of its *meso*-type 2(*R*),7-(*R*),18(*S*),23(*S*)-isomeric macrocycle L1, have been synthesized and characterized by spectroscopic methods. The 2D NMR spectra confirm the identity of these complexes and indicate C_2 symmetry of the $[LnL]^{3+}$ and C_s symmetry of the $[LnL1]^{3+}$ complexes. The crystal structures of the $[PrL(NO_3)(H_2O)_2](NO_3)_2$, $[EuL(NO_3)(H_2O)_2](NO_3)_2$, $[DyL(NO_3)_2]_2[Dy(NO_3)_5]\cdot 5CH_3CN$, $[YbL(NO_3)_2]_2[Yb(NO_3)_5]\cdot 5CH_3CN$, $[YbL(H_2O)_2](NO_3)_3\cdot H_2O$, and $[EuL1(NO_3)(H_2O)_2]_{0.52}[EuL1(NO_3)_2]_{0.48}(NO_3)_{1.52}\cdot 0.48H_2O$ complexes have been determined by single-crystal X-ray diffraction. In all complexes, the lanthanide(III) ions are coordinated by six nitrogen atoms of the macrocycle L or L1, but for each type of complex, the conformation of the macrocycle and the axial ligation are different. The crystallographic, NMR, and CD data show that the $[YbL]^{3+}$ complex exists in two stable forms. Both forms of the Yb(III) complex have been isolated, and their interconversion was studied in various solvents. The two forms of $[YbL]^{3+}$ complex correspond to two diastereomers of ligand L, which differ in the sense of the helical twist and the configuration at the stereogenic amine nitrogen atoms. In one of the stereoisomers, the macrocycle L of (RRRR) configuration at the stereogenic cyclohexane carbon atoms adopts the (RSRS) configuration at the amine nitrogen atoms, while in the other stereoisomer, the macrocycle L of (RRRR) configuration at the stereogenic cyclohexane carbon atoms adopts the (SSSS) configuration at the amine nitrogen atoms. The (RRRR)(RSRS) isomer is quantitatively converting to the (RRRR)(SSSS) isomer in water solution, while the reverse process is observed for an acetonitrile solution, thus representing the rare case of helicity inversion controlled by the solvent.

Introduction

The hexaaza tetraimine and tetraamine macrocycles derived from 2,6-diformyl- or 2,6-diacetylpyridine and diamines form thermodynamically and kinetically stable complexes with the relatively large lanthanide(III) ions.[1] In this way, robust lanthanide complexes may be obtained for potential applications. In particular, Schiff base complexes of this type have been demonstrated to be very efficient catalysts in hydrolytic cleavage of various phosphate esters,[2] including RNA[3] and plasmid DNA.[4] These macrocyclic Schiff base complexes suffer from slow decomposition, most likely, caused by hydrolytic destruction of the imine macrocycle in aqueous solution. It may be expected that application of their amine analogues may overcome the problem of hydrolytic decomposition. In addition, the introduction of chiral, enantiopure ligand such as L (with all-R configuration of the cyclohexane carbon atoms, Scheme 1), may lead to additional interesting effects, for example, dependence of catalytic activity in DNA hydrolysis on the handedness of $[LnL]^{3+}$ complex or kinetic resolution of chiral phosphate triesters.

The synthesis, as well as X-ray crystal structure, of the La(III) complex of the racemic form of macrocycle L was briefly communicated by Bligh and co-workers.[5] In an

* To whom correspondence should be addressed. E-mail: jurekl@wchuwr.chem.uni.wroc.pl. Fax: 48 71 3282348. Tel: 48 71 3757252.

(1) (a) Radecka-Paryzek, W.; Patroniak, V.; Lisowski, J. *Coord. Chem. Rev*. **2005**, *249*, 2156−2175. (b) Vigato, P. A.; Tamburini, S. *Coord. Chem. Rev*. **2004**, *248*, 1717−2128.

(2) Hay, R. W.; Govan, N. *Polyhedron* **1997**, *24*, 4233−4237.

(3) (a) Morrow, J. R.; Buttrey, L. A.; Shelton, V. M.; Berback, K. A. *J. Am. Chem. Soc*. **1992**, *114*, 1903−1905. (b) Hayashi, N.; Takeda, N.; Shiiba, T.; Yashiro, M.; Watanabe, K.; Komiyama, M. *Inorg. Chem.* **1993**, *32*, 5899−5900.

(4) Bligh, S. W. A.; Choi, N.; Evagorou, E. G.; McPartlin, M.; White, K. N. *J. Chem. Soc., Dalton Trans.* **2001**, 3169−3172.

(5) Bligh, S. W. A.; Choi, N.; Evagorou, E. G.; Li, W.-S.; McPartlin M. *Chem. Commun.* **1994**, 2399−2400.

10.1021/ic700831z CCC: $37.00
Published on Web 08/17/2007

Scheme 1. Structures of the Two Isomers of the Chiral Macrocycle L, the *meso*-Macrocycle L1, and the Numbering Scheme

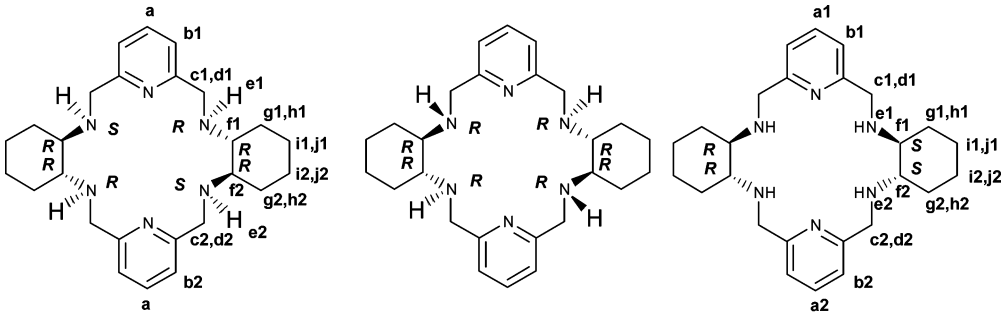

L (RRRR)(RSRS) **L** (RRRR)(RRRR) **L1** (RRSS)

attempt to obtain the analogous enantiopure complexes with various Ln(III) ions, we have unexpectedly found that the synthesis of these compounds is not straightforward and various types of complexes are obtained, depending on the size of Ln(III) ion and the experimental conditions. We have also synthesized the Eu(III) complex of the *meso*-type macrocycle L1, which is an isomer of L differing in configuration at stereogenic carbon atoms (Scheme 1).[6]

In particular, we report here two diastereomers of macrocycle L observed in two forms of the $[YbL]^{3+}$ complex, differing in the configuration at the stereogenic amine nitrogen atoms (Scheme 1). While this type of isomerism is well-known for complexes of tetraazamacrocycles,[7] to the best of our knowledge, we present the first example of this effect for complexes of hexaazamacrocyles. The two forms of Yb(III) complex differ also in the mutual orientation of the pyridine rings, that is, the sense of helical twist of the macrocycle, in a manner similar to that observed for the related 3 + 3 nonaazamacrocyclic Ln(III) complexes.[8] We also present here the selective interconversion of one form into the other, controlled by the kind of solvent used. This effect represents the very rare case of solvent-induced helicity inversion. Controlled inversion of helicity of enantiopure structures,[8−11] triggered, for example, by formation of thermodynamic product, change of redox state, or solvent, is a rare phenomenon, particularly for inorganic systems. It should be noted that the process of helicity inversion attracts a lot of attention in light of the inversion of the normal right-handed helix of B-DNA to the left-handed helix of Z-DNA.[12]

Experimental Section

Measurements. The NMR spectra were taken on Bruker Avance 500 and AMX 300 spectrometers. The chemical shifts were referenced to the residual solvent signal. The gradient COSY, TOCSY, NOESY, ROESY, and HMQC spectra were acquired using 512 × 1K data points and zero filled to a 1K × 1K matrix. Mixing times of 25−200 ms were used in NOESY and ROESY experiments. The CD spectra were measured on a Jasco J-715 spectropolarimeter. The electrospray mass spectra of methanol solutions containing traces of HCOOH were obtained using Bruker microOTOF-Q instrument. The elemental analyses were carried out on a Perkin-Elmer 2400 CHN elemental analyzer.

Crystal Structure Determination. The isomorphous crystals of $[PrL(NO_3)(H_2O)_2](NO_3)_2$ and $[EuL(NO_3)(H_2O)_2](NO_3)_2$ suitable for single-crystal X-ray diffraction experiments were obtained by slow evaporation of methanol/acetonitrile solutions of the $[PrL](NO_3)_3 \cdot 0.5H_2O$ and $[EuL](NO_3)_3 \cdot 3H_2O$ complexes, respectively. The isomorphous crystals of $[DyL(NO_3)_2]_2[Dy(NO_3)_5] \cdot 5CH_3CN$ and $[YbL(NO_3)_2]_2[Yb(NO_3)_5](NO_3)_4 \cdot 5CH_3CN$ were grown by slow evaporation of acetonitrile solutions of the $[DyL]_2[Dy(NO_3)_5](NO_3)_4 \cdot H_2O$ and $[YbL]_2[Yb(NO_3)_5](NO_3)_4 \cdot 2H_2O$ complexes, respectively. Crystals of $[YbL(H_2O)_2](NO_3)_3 \cdot H_2O$ were obtained by slow evaporation of a water solution of the $[YbL(H_2O)_2](NO_3)_3$ complex. Crystals of $[EuL1(NO_3)(H_2O)_2]_{0.52}[EuL1(NO_3)_2]_{0.48}(NO_3)_{1.52} \cdot 0.48H_2O$ were grown by slow evaporation of a methanol/chloroform solution of the $[EuL1](NO_3)_3 \cdot CH_3OH \cdot H_2O$ complex.

The crystallographic measurements were performed on κ-geometry Kuma KM4CCD automated four-circle diffractometers (ω scan) with graphite-monochromatized Mo Kα radiation. The data for the crystals were collected at 100(2) K. A summary of the conditions for the data collection and the structure refinement parameters are given in Table 1. The data were corrected for Lorentz and

(6) Gregoliński, J.; Lisowski, J.; Lis, T. *Org. Biomol. Chem*. **2005**, *3*, 3161−3166.

(7) For example, see: (a) El Ghachtouli, S.; Cadiou, C.; Déchamps-Olivier, I.; Chuburu, F.; Aplincourt, M.; Roisnel, T. *Eur. J. Inorg. Chem.* **2006**, 3472−3481. (b) Bucher, C.; Moutet, J. C.; Pécaut, J.; Royal, G.; Saint-Aman, E.; Thomas, F.; Torelli, S.; Ungureanu, M. *Inorg. Chem.* **2003**, *42*, 2242−2252. (c) Bucher, C.; Moutet, J.-C.; Pécaut, J.; Royal, G.; Saint-Aman, E.; Thomas, F. *Inorg. Chem.* **2004**, *43*, 3777−3779. (d) Bosnich, B.; Tobe, M. L.; Webb, G. A. *Inorg. Chem.* **1965**, *4*, 1109−1112. (e) Creutz, C.; Chou, M. H.; Fujita, E.; Szalda, D. J. *Coord. Chem. Rev.* **2005**, *249*, 375−390. (f) Liang, X.; Sadler, P. J. *Chem. Soc. Rev.* **2004**, *33*, 246−266. (g) Madej, E.; Monsted, O.; Kita, P. *J. Chem. Soc., Dalton Trans* **2002**, 2361−2365. (h) Haines, R. I.; Hutchings, D. R.; McCormack, T. M. *J. Inorg. Biochem.* **2001**, *85*, 1−7. (i) Curtis, N. F. *Inorg. Chim. Acta* **2001**, *317*, 27−32. (j) Slocik, J. M.; Ward, M. S.; Shepherd, R. E. *Inorg. Chim. Acta* **2001**, *317*, 290−303.

(8) Gregoliński, J.; Lisowski, J. *Angew. Chem., Int. Ed*. **2006**, *45*, 6122−6126.

(9) For controlled helicity inversion related to coordination chemistry, see: (a) Miyake, H.; Sugimoto, H.; Tamiaki, H.; Tsukube, H. *Chem. Commun*. **2005**, 4291−4293. (b) Miyake, H.; Yoshida, K.; Sugimoto, H.; Tsukube, H. *J. Am. Chem. Soc*. **2004**, *126*, 6524−6525. (c) Hutin, M.; Nitschke, J. *Chem. Commun*. **2006**, 1724−1726. (d) Zahn, S.; Canary, J. W. *Science* **2000**, *288*, 1404−1407. (e) Zahn, S.; Das, D.; Canary, J. W. *Inorg. Chem*. **2006**, *45*, 6056−6063.(f) Biscarini, P.; Kuroda, R. *Inorg. Chim. Acta* **1988**, *154*, 209−214.

(10) For controlled helicity inversion in organic polymeric systems, see: (a) Okoshi, K.; Sakurai, S.-i.; Ohsawa, S.; Kumaki, J.; Yashima, E. *Angew. Chem., Int. Ed.* **2006**, *45*, 8173−8176. (b) Sakurai, S.-i.; Okoshi, K.; Kumaki, J.; Yashima, E. *J. Am. Chem. Soc*. **2006**, *128*, 5650−5651. (c) Tang, H.-Z.; Novak, B. M.; He, J.; Polavarapu, P. L. *Angew. Chem., Int. Ed.* **2005**, *44*, 7298−7301. (d) Ajayaghosh, A.; Varghese, R.; George, S. J.; Vijayakumar, C. *Angew. Chem., Int. Ed.* **2006**, *45*, 1141−1144. (e) Lohr, A.; Lysetska, M.; Würthner, F. *Angew. Chem., Int. Ed.* **2005**, *44*, 5071−5074.

(11) Borovkov, V. V.; Hembury, G. A.; Inoue, Y. *Angew. Chem., Int. Ed.* **2003**, *42*, 5310−5314.

(12) Belmont, P.; Constant, J.-F.; Demeunynck, M. *Chem. Soc. Rev*. **2001**, *30*, 70−81.

Table 1. Crystallographic Data of the Complexes

	$[PrL(NO_3)(H_2O)_2](NO_3)_2$	$[EuL(NO_3)(H_2O)_2](NO_3)_2$	$[DyL(NO_3)_2]_2[Dy(NO_3)_5]\cdot 5CH_3CN$	$[YbL(NO_3)_2]_2[Yb(NO_3)_5]\cdot 5CH_3CN$	$[YbL(H_2O)_2](NO_3)_3\cdot H_2O$	$[EuL1(NO_3)(H_2O)_2]_{0.52}[EuL1(NO_3)_2]_{0.48}(NO_3)_{1.52}\cdot 0.48H_2O$
empirical formula	$C_{26}H_{42}N_9O_{11}Pr$	$C_{26}H_{42}EuN_9O_{11}$	$C_{62}H_{91}Dy_3N_{26}O_{27}$	$C_{62}H_{91}N_{26}O_{27}Yb_3$	$C_{26}H_{44}N_9O_{12}Yb$	$C_{26}H_{41.04}EuN_9O_{10.52}$
fw (g mol^{-1})	797.60	808.65	2120.11	2151.73	847.74	799.64
cryst syst	monoclinic	monoclinic	monoclinic	monoclinic	orthorhombic	triclinic
space group	$P2_1$ (No. 4)	$P2_1$ (No. 4)	$P2_1$ (No. 4)	$P2_1$ (No. 4)	$P2_12_12_1$ (No. 19)	$P\bar{1}$ (No. 2)
a (Å)	14.408(3)	14.292(3)	11.980(3)	11.924(3)	10.701(3)	11.139(3)
b (Å)	15.040(3)	15.103(3)	16.215(4)	16.270(4)	12.479(3)	12.052(3)
c (Å)	15.586(3)	15.524(3)	21.707(4)	21.642(4)	24.070(5)	13.872(3)
α (deg)						87.57(3)
β (deg)	105.15(3)	105.52(3)	105.49(3)	105.47(3)		67.35(3)
γ (deg)						64.37(3)
V (Å^3)	3260.0(11)	3228.7(11)	4063.5(16)	4046.5(16)	3214.3(14)	1532.2(7)
Z	4	4	2	2	4	2
T (K)	100(2)	100(2)	100(2)	100(2)	100(2)	100(2)
D_{calcd} (g cm^{-3})	1.625	1.664	1.733	1.766	1.752	1.734
μ (mm^{-1})	1.566	2.014	2.823	3.532	2.986	2.120
cryst size (mm)	0.20 × 0.18 × 0.16	0.43 × 0.27 × 0.26	0.20 × 0.17 × 0.14	0.37 × 0.16 × 0.10	0.55 × 0.12 × 0.08	0.23 × 0.09 × 0.09
radiation type	Mo Kα	Mo Kα	Mo Kα	Mo Kα	Mo Kα	Mo Kα
λ (Å)	0.71073	0.71073	0.71073	0.71073	0.71073	0.71073
θ range (deg)	3.03−26.00	3.04−26.00	3.07−26.00	2.99−26.00	3.02−25.99	3.22−26.00
index ranges	$-17 \le h \le 17$ $-18 \le k \le 15$ $-19 \le l \le 19$	$-17 \le h \le 17$ $-18 \le k \le 18$ $-16 \le l \le 19$	$-14 \le h \le 14$ $-17 \le k \le 20$ $-26 \le l \le 26$	$-14 \le h \le 14$ $-20 \le k \le 20$ $-24 \le l \le 26$	$-13 \le h \le 9$ $-15 \le k \le 15$ $-29 \le l \le 29$	$-13 \le h \le 13$ $-14 \le k \le 14$ $-16 \le l \le 17$
T_{min}/T_{max}	0.745/0.819	0.516/0.700	0.494/0.614	0.447/0.701	0.373/0.798	0.682/0.859
measured reflns	32 831	29 828	30 412	48 779	35 992	13 298
independent reflns	10 493	12 240	12 281	15 375	6305	5989
obsd reflns ($I > 2\sigma(I)$)	9592	11 559	10 738	14 440	6036	4913
R_{int}	0.0441	0.0309	0.0511	0.0522	0.0421	0.0374
data/restraints/params	10 493/13/872	12 240/13/875	12 281/1/1068	15 375/1/1068	6305/0/456	5989/6/456
R1, wR2[a] ($F_o^2 > 2\sigma(F_o^2)$)	0.0287, 0.0458	0.0215, 0.0484	0.0342, 0.0615	0.0328, 0.0743	0.0183, 0.0377	0.0283, 0.0412
R1, wR2 (all data)	0.0347, 0.0468	0.0237, 0.0490	0.0429, 0.0633	0.0363, 0.0754	0.0204, 0.0380	0.0432, 0.0428
GOF = S	1.009	1.038	1.002	1.012	1.010	1.014
$\Delta\rho_{max}/\Delta\rho_{min}$ (e Å^{-3})	0.50/−0.57	0.89/−0.80	1.34/−0.49	1.06/−0.75	0.77/−0.58	0.74/−0.62

[a] $R1 = \sum||F_0| - |F_c|| / \sum|F_0|$; $wR2 = \sqrt{\sum[w(F_0^2-F_c^2)^2]/\sum[w(F_0^2)^2]}$. Detailed values of the weighing scheme (w) in each system are given in the crystallographic information file (CIF) provided as Supporting Information.

polarization effects, and an analytical absorption correction was applied. Data collection, cell refinement, data reduction and analysis were carried out with KM4CCD software (Oxford Diffraction, Poland), CrysAlis CCD, and CrysAlis RED, respectively.[13] The structures of europium and ytterbium complexes were solved by direct methods using the SHELXS-97 program[14] and refined on F^2 by a full-matrix least-squares technique using SHELXL-97[15] with anisotropic thermal parameters for all ordered and fully occupied non-H atom positions. Some of the not fully occupied positions in $[EuL1(NO_3)(H_2O)_2]_{0.52}[EuL1(NO_3)_2]_{0.48}(NO_3)_{1.52}\cdot 0.48H_2O$ were also refined anisotropically. $[EuL(NO_3)(H_2O)_2](NO_3)_2$ and $[PrL(NO_3)(H_2O)_2](NO_3)_2$ are isomorphous, so the refinement for the latter was started by using the coordinates for ordered heavy atoms of the former. The same was done for the other pair of isomorphous crystals: $[YbL(NO_3)_2]_2[Yb(NO_3)_5]\cdot 5CH_3CN$ and $[DyL(NO_3)_2]_2[Dy(NO_3)_5]\cdot 5CH_3CN$. All figures were made with the XP,[16] Mercury,[17] and Ortep3[18] programs.

All N- and C-bonded hydrogen atoms were included from geometry and were treated as riding atoms with N−H distances of 0.93 Å, C−H distances of 0.95−1.00 Å, and U_{iso} values of $1.2U_{eq}$(N,C) for the NH, CH, and CH_2 groups and $U_{iso} = 1.5U_{eq}$(C) for the CH_3 groups. Water H atoms in $[EuL(NO_3)(H_2O)_2](NO_3)_2$, $[PrL(NO_3)(H_2O)_2](NO_3)_2$, and $[YbL(H_2O)_2](NO_3)_3\cdot H_2O$ were found in difference Fourier maps and were refined isotropically. H1W in $[PrL(NO_3)(H_2O)_2](NO_3)_2$ and H2W in $[YbL(H_2O)_2](NO_3)_3\cdot H_2O$ were refined with $U_{iso} = U_{eq}$(O1W). H2W, H5W, and H7W in $[PrL(NO_3)(H_2O)_2](NO_3)_2$ and H2W in $[EuL(NO_3)(H_2O)_2](NO_3)_2$ were

(13) *KM4CCD Software: CRYSALIS CCD and CRYSALIS RED*, version 1.171; Oxford Diffraction: Wroclaw, Poland, 1995−2003.
(14) Sheldrick, G. M. *SHELXS-97, Program for the Solution of Crystal Structures*; University of Göttingen: Göttingen, Germany, 1997.
(15) Sheldrick, G. M. *SHELXL-97, Program for the Refinement of Crystal Structuresz*; University of Göttingen: Göttingen, Germany, 1997.
(16) *XP−Interactive Molecular Graphics*, version 5.1; Bruker Analytical *X*-ray Systems: Madison, WI, 1998.
(17) *MERCURY, Programme for Crystal Structure Visualisation and Exploration*, version 1.4.1; CCDC, Cambridge University: Cambridge, U.K., 2005.
(18) Farrugia, L. J. ORTEP-3 for Windows. *J. Appl. Cryst.* **1997**, *30*, 565.

refined with $U_{iso} = 1.5U_{eq}(O)$. O−H distances in all the water molecules in $[PrL(NO_3)(H_2O)_2](NO_3)_2$ and $[EuL(NO_3)(H_2O)_2](NO_3)_2$ were constrained to 0.86 Å. Water H atoms from not fully occupied water positions in $[EuL1(NO_3)(H_2O)_2]_{0.52}[EuL1(NO_3)_2]_{0.48}(NO_3)_{1.52}\cdot 0.48H_2O$ were not found in difference Fourier maps.

One of the six NO_3^- groups located in both $[PrL(NO_3)(H_2O)_2](NO_3)_2$ and $[EuL(NO_3)(H_2O)_2](NO_3)_2$ (denoted as N17) is disordered into two positions with sof = 0.64(3) and 0.36(3) in $[PrL(NO_3)(H_2O)_2](NO_3)_2$ and 0.57(2) and 0.43(2) in $[EuL(NO_3)(H_2O)_2](NO_3)_2$. Disordered atom positions were refined isotropically.

The crystal of europium complex of *meso*-L1 is of a solid solution type. Two different complex cations may be distinguished in the same, symmetrically equivalent position: $[EuL1(NO_3)(H_2O)_2]^{2+}$ with sof = 0.525(4) and $[EuL1(NO_3)_2]^+$ with sof = 0.475(4). Additionally, the disorder of the complex cation is correlated with the disorder of the uncoordinated NO_3^- ions (N8 with sof = 0.525(4) and N10 disordered into two positions with sof = 0.525(4) and 0.475(4)) and one water molecule (O3W, sof = 0.475(4)). Therefore, in the final model, the formula $[EuL1(NO_3)(H_2O)_2]_{0.52}[EuL1(NO_3)_2]_{0.48}(NO_3)_{1.52}\cdot 0.48H_2O$ corresponds to the existence of two complexes, $[EuL1(NO_3)(H_2O)_2](NO_3)_2$ and $[EuL1(NO_3)_2](NO_3)\cdot H_2O$, randomly occupying the crystallographic sites of the unit cell in a 0.52:0.48 ratio. In the refinement procedure, equivalent bond distances and angles within two positions of disordered N10 NO_3^- group were restrained to be equal with the use of SAME instruction.

Syntheses. Macrocycle **L1** was obtained as previously described.[6]

Macrocycle **L** was obtained by the modification of the literature method.[19] The solution of 5 mmol (2.222 g) of $Sm(NO_3)_3\cdot 6H_2O$ and 10 mmol (1.351 g) of 2,6-diformylpyridine in 100 mL of methanol was combined with the solution of 10 mmol (1.142 g) of *trans*-(1*R*,2*R*)-diaminecyclohexane in 50 mL of methanol. The mixture was refluxed for 4 h, and the resulting suspension of macrocyclic Schiff base complex was cooled down. The mixture was placed in an ice bath; an excess of $NaBH_4$ (4.54 g) was gradually added to the stirred solution for 2 h, and the solution was stirred for 2 h at room temperature. The solvent was evaporated to dryness; the residue was combined with 500 mL of a 10% solution of H_2SO_4, and the obtained solution was heated 48h at 70 °C. The mixture was cooled down and neutralized on an ice bath with NaOH until pH 11−12. The precipitated mixture of $Sm(OH)_3$ and amine L was filtered, and the product was extracted with 50 mL of methanol. The methanol and water filtrates were combined; methanol was removed on rotary evaporator, and the remaining water solution was extracted with 5 × 80 mL of chloroform, dried over anhydrous Na_2SO_4, and evaporated to dryness to give 1.875 g of crude macrocycle L. The product was dissolved in 25 mL of ethanol; 6 mL of 48% HBr solutions was added, and the obtained solution was evaporated to dryness under reduced pressure. The residue was dissolved in 25 mL of ethanol; the volume was reduced to 1/4, and the solution was left in the freezer overnight. The obtained precipitate was filtered, washed with cold ethanol, and dried. The hydrobromide derivative was dissolved in 20 mL of water, and solid NaOH was added until pH 12. The solution was extracted 3 times with10 mL of chloroform, dried over anhydrous Na_2SO_4, and evaporated to dryness to give 1.40 g (64%) of macrocycle L. ESI-MS: *m*/*z* 435.3 $C_{26}H_{39}N_6^+$, 457.3 $C_{26}H_{38}N_6Na^+$. ^{1}H NMR (500 MHz, $CDCl_3$): δ 7.53 (2H, t), 7.03 (4H, d), 4.05 (4H, d), 3,77 (4H, d), 3.52 (4H, broad), 2.08 (4H, m), 2.05 (4H, m), 1.63 (4H, m), 1.10 (4H, m), 1.03 (4H, m). Anal. Calcd (found) for $C_{26}H_{39}N_6O_{0.5}$: C, 70.39 (68.96); H, 8.86 (8.47); N, 18.94 (19.19).

$[LnL]_2[Ln(NO_3)_5](NO_3)_4$. A solution of 0.2 mmol of the appropriate lanthanide(III) nitrate hydrate in 3 mL of acetonitrile was combined with the solution of 0.2 mmol (86.9 mg) of amine L in 3 mL of dichloromethane and refluxed for 4 h. The mixture was filtered, evaporated to dryness, redissolved in the mixture of 3 mL of acetonitrile and 3 mL of dichloromethane, and concentrated to ∼1 mL, when precipitate appeared. The mixture was left overnight in a freezer, and the obtained precipitate was filtered, washed with small amount of cold acetonitrile, and dried.

$[YbL]_2[Yb(NO_3)_5](NO_3)_4\cdot 2H_2O$. Yield: 73.8 mg (37.24% based on L). ESI-MS: *m*/*z* 732.2 $\{[YbL](NO_3)_2\}^+$, 715.2 $\{[YbL](NO_3)(HCOO)\}^+$, 335.1 $\{[YbL](NO_3)\}^{+2}$. ^{1}H NMR (500 MHz, $CDCl_3$/CD_3OD v/v 2/1, 298 K): δ −119.17, −74.71, −40.73, −36.82, −29.35, −28.28, −27.97, −24.43, −23.44, −17.52, −10.78, −9.65, −8.79, −6.55, −4.56, −0.58, 1.32, 3.64, 6.23. ^{1}H NMR (500 MHz, CD_3CN, 298 K): δ −134.96, −75.60, −40.55, −37.98, −30.39, −30.26, −28.64, −25.77, −24.15, −18.01, −10.33, −8.21, −6.72, −6.41, −4.84, −1.65, 1.58, 3.81, 6.04. ^{1}H NMR (500 MHz, D_2O, 298 K): δ −74.88, −60.35, −47.47, −44.02, −40.97, −33.76, −27.48, −14.15, −13.04, −11.68, −11.60, −7.45, −7.03, −1.96, 7.16, 10.02, 25.03, 29.75, 84.10. Anal. Calcd (found) for $Yb_3C_{52}H_{80}N_{21}O_{29}$: C, 31.27 (31.51); H, 3.80 (4.07); N, 14.70 (14.84). CD [H_2O, λ_{max}/nm (ϵ/M^{-1} cm^{-1})]: 194 (−4), 234 (2), 250 (1), 272 (3). CD [CH_3CN, λ_{max}/nm (ϵ/M^{-1} cm^{-1})]: 205 (−23), 246 (0), 270 (−9).

$[DyL]_2[Dy(NO_3)_5](NO_3)_4\cdot H_2O$. Yield: 57.1 mg (29.56% based on L). ESI-MS: *m*/*z* 722.2 $\{[DyL](NO_3)\}_2^+$, 705.2 $\{[DyL](NO_3)(HCOO)\}^+$. ^{1}H NMR (500 MHz, $CDCl_3$/CD_3OD v/v 2/1, 298 K): δ −4.18, 7.46, 33.29, 34.57, 37.48, 40.60, 46.14, 50.67, 54.20, 77.96, 92.92, 115.81, 123.36, 142.79, 172.67, 177.75, 314.92. ^{1}H NMR (500 MHz, CD_3CN, 298 K): δ −22.63, −2.15, −0.83, 2.61, 6.60, 32.88, 34.51, 37.74, 44.26, 47.69, 56.41, 79.64, 88.79, 97.95, 132.61, 150.03, 187.30, 193.37, 319.68. Anal. Calcd (found) for $Dy_3C_{52}H_{78}N_{21}O_{28}$: C, 32.35 (32.31); H, 4.26 (4.07); N, 15.19 (15.22). CD [CH_3CN, λ_{max}/nm (ϵ/M^{-1} cm^{-1})]: 204 (−27), 246 (−1), 271 (−9).

$[TbL]_2[Tb(NO_3)_5](NO_3)_4\cdot 3H_2O$. Yield: 57.1 mg (29.2% based on L). ESI-MS: *m*/*z* 717.2 $\{[TbL](NO_3)_2\}^+$, 700.2 $\{[Tb\mathbf{L}](NO_3)(HCOO)\}^+$. ^{1}H NMR (500 MHz, $CDCl_3$/CD_3OD v/v 2/1, 298 K): δ −3.74, −2.12, −0.21, 15.18, 17.27, 28.04, 31.37, 35.66, 40.45, 60.55, 72.39, 75.51, 89.96, 92.50, 102.00, 122.26, 245.45. ^{1}H NMR (500 MHz, CD_3CN, 298 K): δ −8.98, −1.08, 0.77, 4.30, 21.79, 23.85, 27.16, 28.33, 40.71, 46.92, 53.70, 57.78, 59.60, 71.69, 99.06, 110.34, 121.07, 145.33, 231.95. Anal. Calcd (found) for $Tb_3C_{52}H_{82}N_{21}O_{30}$: C, 32.35 (31.90); H, 4.29 (4.22); N, 14.63 (15.02). CD [CH_3CN, λ_{max}/nm (ϵ/M^{-1} cm^{-1})]: 204 (−29), 246 (−1), 271 (−10).

$[EuL]_2[Eu(NO_3)_5](NO_3)_4\cdot 3CH_3CN$. Yield: 102.7 mg (51.2% based on L). ESI-MS: *m*/*z* 711.2 $\{[EuL](NO_3)_2\}^+$, 694.2 $\{[EuL](NO_3)(HCOO)\}^+$. ^{1}H NMR (500 MHz, $CDCl_3$/CD_3OD v/v 2/1, 298 K): δ −30.75, −29.82, −24.64, −17.86, −10.20, −9.87, −8.62, −5.58, −5.44, −4.84, −4.58, −2.89, −1.62, −1.37, −0.83, 0.65, 3.92, 5.84, 28.65. ^{1}H NMR (500 MHz, CD_3CN, 298 K): δ −31.84, −31.10, −24.55, −16.78, −10.76, −10.18, −8.94, −5.43, −5.32, −4.68, −3.89, −2.89, −1.71, −1.69, −0.55, 0.73, 4.31, 6.03, 30.13. Anal. Calcd (found) for $Eu_3C_{58}H_{85}N_{24}O_{27}$: C, 34.93 (34.72); H, 4.22 (4.27); N, 16.82 (16.75). CD [CH_3CN, λ_{max}/nm (ϵ/M^{-1} cm^{-1})]: 204 (−31), 246 (−1), 271 (−10).

$[YbL][Yb(NO_3)_5](NO_3)\cdot CH_3CN$. The solution of 0.3 mmol (134.7 mg) of $Yb(NO_3)_3\cdot 5H_2O$ in 3 mL of acetonitrile was

(19) Fitzsimmons, P. M.; Jackels, S. C. *Inorg. Chim. Acta* **1996**, *246*, 301−310.

combined with solution of 0.2 mmol (86.9 mg) of amine L in 3 mL of dichloromethane and refluxed for 4 h. The solution was cooled, filtered, and concentrated to ~1−2 mL, until precipitate appeared. The mixture was left in a refrigerator for 1 h, and the obtained creamy precipitate was filtered, washed with small amount of cold acetonitrile, and dried under vacuum to give 80.1 mg (33.5% based on L) of complex. Anal. Calcd (found) for $Yb_2C_{28}H_{41}N_{13}O_{18}$: C, 28.30 (28.17); H, 3.59 (3.46); N, 15.51 (15.25). The ^{1}H NMR spectra are practically identical to that of the $[YbL]_2[Yb(NO_3)_5](NO_3)_4\cdot 2H_2O$ complex.

$[YbL(H_2O)_2](NO_3)_3$. $Yb(NO_3)_3\cdot 5H_2O$ (0.5 mmol, 224.7 mg) and macrocycle L (0.5 mmol, 217.3 mg) were suspended in 20 mL of water, and the mixture was heated at 80 °C for 90 min. The obtained clear solution was concentrated to ~5 mL and left overnight in a fridge. The obtained precipitate was filtered and dried in vacuum to give 220.3 mg (55.5%) of a white product. ESI-MS: *m*/*z* 732.2 $\{[YbL](NO_3)_2\}^+$, 715.2 $\{[YbL](NO_3)(HCOO)\}^+$, 335.1 $\{[YbL](NO_3)\}^{+2}$. ^{1}H NMR (500 MHz, CD_3CN, 298 K): δ −107.49, −82.39, −58.77, −54.32, −32.77, −20.03, −15.38, −11.83, −8.43, −5.32, −1.05, 4.09, 6.78, 12.65, 16.96, 20.32, 34.54, 38.86, 49.16. ^{1}H NMR (500 MHz, D_2O, 298 K): δ −75.41, −74.47, −71.49, −68.90, −25.28, −21.62, −9.87, −2.36, −2.26, 1.08, 3.41, 5.44, 12.55, 16.76, 18.09, 24.00, 40.14, 48.28, 102.29. Anal. Calcd (found) for $YbC_{26}H_{38}N_9O_9$: C, 39.00 (39.35); H, 4.88 (4.83); N, 16.04 (15,88). CD [H_2O, λ_{max}/nm (ϵ/M^{-1} cm^{-1})]: 189 (28), 203 (−4), 218 (2), 266 (13). CD [CH_3CN, λ_{max}/nm (ϵ/M^{-1} cm^{-1})]: 194 (22), 268 nm (−7).

$[LnL](NO_3)_3$. The appropriate lanthanide(III) nitrate hydrate (0.2 mmol) and amine L (0.2 mmol, 86.9 mg) were dissolved in 8.5 mL of isopropanol and refluxed for 2 h. The formed white precipitate was filtered and redissolved in in 5 mL of acetonirile. The solution was concentrated until precipitate appeared. The mixture was left overnight in a freezer, and the obtained precipitate was filtered, washed with small amount of cold acetonitrile, and dried.

$[DyL](NO_3)_3$. Yield: 86.3 mg (55.1%) of white product. Anal. Calcd (found) for $DyC_{26}H_{38}N_9O_9$: C, 39.70 (39.88); H, 4.71 (4.89); N, 16.01 (16.10). ^{1}H NMR spectra are practically identical to that of the $[DyL]_2[Dy(NO_3)_5](NO_3)_4\cdot H_2O$ complex.

$[EuL](NO_3)_3\cdot 3H_2O$. Yield: 94.1 mg (56.9% based on L). Anal. Calcd (found) for $EuC_{26}H_{44}N_9O_{12}$: C, 37.62 (37.78); H, 4.99 (5.36); N, 15.37 (15.25). ^{1}H NMR spectra are practically identical to that of the $[EuL]_2[Eu(NO_3)_5](NO_3)_4\cdot 3CH_3CN$ complex.

$[LnL](NO_3)_3$. A solution of 0.2 mmol (87.7 mg) of the appropriate lanthanide(III) nitrate hydrate in 3 mL of acetonitrile was combined with a solution of 0.2 mmol (86.9 mg) of amine L in 3 mL of dichloromethane and refluxed for 4 h. The solution was cooled down and evaporated to dryness. The residue was redissolved in 3 mL of acetonitrile, and the solution was concentrated until a precipitate appeared. The mixture was left overnight in a freezer, and the obtained precipitate was filtered, washed with small amount of cold acetonitrile, and dried.

$[NdL](NO_3)_3\cdot 1.5H_2O$. Yield: 39.8 mg (25.2%) of pinkish product. An additional crop of the product was obtained by precipitation of the filtrate with diethyl ether: 51.1 mg (32.3%). ESI-MS: *m*/*z* 700.2 $\{[NdL](NO_3)_2\}^+$, 683.2 $\{[NdL](NO_3)(HCOO)\}^+$. ^{1}H NMR (500 MHz, $CDCl_3/CD_3OH$ v/v 2/1, 298 K): δ −14.82, 4.25, 4,67, 5.40, 6.85, 6.96, 6.99, 7.18, 7.50, 8.22, 11.05, 11.15, 11.78, 12.95, 13.13, 16.58, 25.54, 27.17, 36.69. ^{1}H NMR (500 MHz, CD_3CN, 298 K): −21.44, 3.16, 3.80, 4.54, 5.10, 6.38, 6.42, 6.93, 7.02, 8.14, 10.06, 10.32, 11.61, 12.48, 13.83, 19.10, 25.91, 28.66, 40.07. Anal. Calcd (found) for $NdC_{26}H_{41}N_9O_{10,5}$: C, 39.32 (39.43); H, 4.90 (5.22); N, 15.81 (15.92). CD [CH_3CN, λ_{max}/nm (ϵ/M^{-1} cm^{-1})]: 205 (−35), 244 (−1), 271 (−10).

$[PrL](NO_3)_3\cdot 0.5H_2O$. Yield: 13.4 mg (18.95%) of greenish product. An additional crop of the product was obtained by precipitation of the filtrate with diethyl ether: 119.4 mg (77.5%). ESI-MS: *m*/*z* 699.2 $\{[PrL](NO_3)_2\}^+$, 682.2 $\{[PrL](NO_3)(HCOO)\}^+$, 665.2 $\{[PrL](HCOO)_2\}^+$. ^{1}H NMR (500 MHz, $CDCl_3/CD_3OH$ v/v 2/1, 298 K): δ −5.34, 5.72, 6.32, 6.32, 8.11, 8.44, 8.77, 9.14, 10.27, 10.64, 12.16, 13.51, 14.78, 15.23, 16.21, 17.51, 29.00, 31.93, 52.73. ^{1}H NMR (500 MHz, CD_3CN, 298 K): δ −12.87, 5.26, 5.72, 6.11, 7.32, 7.44, 8.27, 8.95, 8.95, 9.71, 12.41, 12.66, 13.08, 15.74, 17.20, 20.59, 30.90, 32.98, 58.37. Anal. Calcd (found) for $PrC_{26}H_{39}N_9O_{9.5}$: C, 40.79 (40.53); H, 4.92 (5.10); N, 16.19 (16.36). CD [CH_3CN, λ_{max}/nm (ϵ/M^{-1} cm^{-1})]: 206 (−36), 246 (0), 272 (−9).

$[EuL1](NO_3)_3\cdot CH_3OH\cdot H_2O$. The solution of 0.1 mmol (42.7 mg) of $Eu(NO_3)_3\cdot 5H_2O$ in 5 mL of acetonitrile was combined with the solution of 0.1 mmol (43.4 mg) of amine L1 in 5 mL of dichloromethane and refluxed for 4 h. The clear solution was evaporated to dryness; the residue was redissolved in 5 mL of methanol and slowly concentrated on rotary evaporator to ~2 mL, until a precipitate appeared. The mixture was left overnight in a freezer, and the obtained precipitate was filtered, washed with small amount of cold methanol, and dried to give 48 mg (58.4%) of product. ESI-MS: *m*/*z* 711.2 $\{[EuL1](NO_3)_2\}^+$, 694.2 $\{[EuL1](NO_3)(HCOO)\}^+$, 684.2 $\{[EuL1](NO_3)Cl\}^+$. ^{1}H NMR (500 MHz, CD_3CN, 298 K): δ −26.60, −25.71, −22.76, −11.67, −8.26, −6.92, −6.28, −6.14, −5.76, −5.12, −4.07, −3.95, −3.33,- 1.46, −0.42, 0.34, 0.36, 2.00, 4.07, 6.14. ^{1}H NMR (500 MHz, $CDCl_3/CD_3OH$ v/v 2/1, 298 K): δ −26.81, −26.17, −22.94, −12.10, −8.26, −7.38, −6.20, −6.07, −5.56, −5.11, −3.93, −3.83, −3.24, −1.24, 0.25, 0.42, 1.54, 1.60, 3.98, 5.84. Anal. Calcd (found) for $EuC_{27}H_{44}N_9O_{11}$: C, 39.70 (39.42); H, 5.46 (5.39); N, 15.06 (15.32).

Results and Discussion

Synthesis and Solution Characterization of the Complexes. The $[LnL](NO_3)_3\cdot nH_2O$ complexes exhibit good solubility in water and polar organic solvents, and often, the crude samples did not exhibit tendency to crystallize and to give pure products. On the other hand, the derivatives with complex counteranions, such as $[LnL]_2[Ln(NO_3)_5](NO_3)_4$, exhibit much lower solubility and a higher tendency to crystallize. The synthesis of the lanthanide(III) complexes of macrocycle L depends on the size of Ln(III) ion and experimental conditions. While the solution NMR studies of complexation of L by Ln(III) ions showed successful incorporation of the metal ion in the macrocycle, the isolation of pure complexes presented some problems and was not successful for each Ln(III) ion. It should be noted that the formula of the isolated complex does not always correspond to the starting metal/ligand ratio. The NMR and mass spectra of the $[LnL](NO_3)_3\cdot nH_2O$ and $[LnL]_x[Ln(NO_3)_5]_y(NO_3)_{3x-2y}$ derivatives for the same Ln(III) ions are practically identical, indicating the presence of the same cationic complex in solution. In many cases, however, the ^{1}H NMR spectra of crude reaction mixtures or complexes generated in situ in NMR tubes show mixtures of macrocyclic Ln(III) complexes because of the presence of different stereoisomers of the complexed macrocycle L (vide infra), formation of hydroxo species, or both.

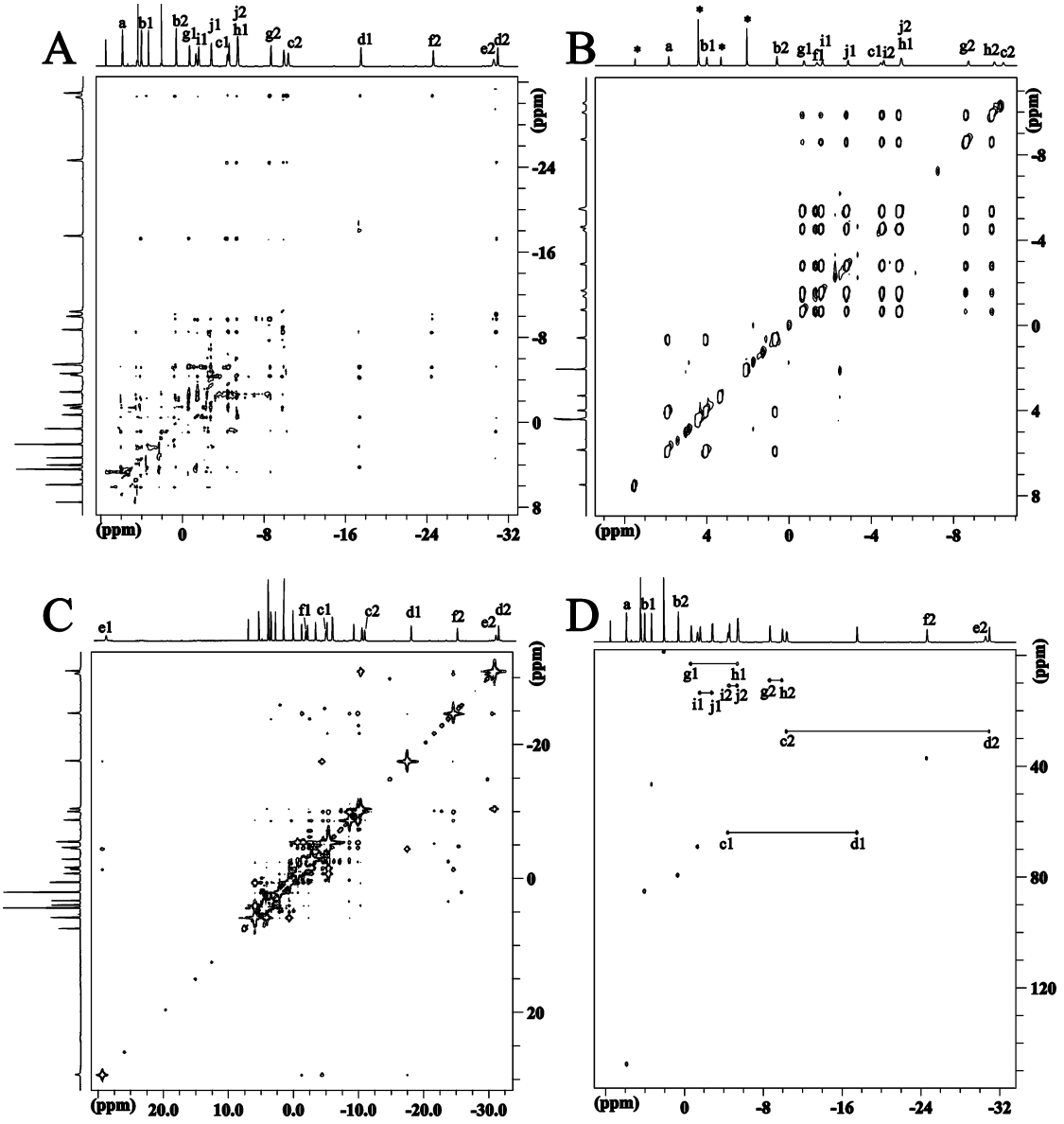

Figure 1. NOESY (A), TOCSY (B), COSY (C), and HMQC (D) spectra of the $[EuL]_2[Eu(NO_3)_5](NO_3)_4 \cdot 3CH_3CN$ complex ($CD_3OD/CDCl_3$ 1:2 v/v solution, 298 K).

The identity of the complexes has been confirmed by elemental analyses and mass spectra. The ESI-MS+ spectra (Supporting Figure S1) of methanol solutions of the complexes show peaks at *m*/*e* corresponding to ions $[LnL](X)^{+2}$ and $[LnL](X)_2^+$, where X is nitrate or anions derived from the solvent used.

The ^{1}H NMR spectra confirm the purity of the isolated complexes. In the case of the Eu(III) and Nd(III) complexes, the lines were assigned on the basis of COSY, TOCSY, NOESY, ROESY, and HMQC measurements (Figure 1). The assignment of the NMR spectra of the Eu(III) complex starts with the analysis of TOCSY spectrum, which identifies the spin systems of the ten cyclohexane protons and the three pyridine protons. The HMQC spectrum identifies the pairs of geminal protons, the two cyclohexane NC*H* positions **f** (see Scheme 1 for labeling), and the resonances of NH groups. The analysis of COSY correlations allows for finding of signal of pyridine γ-proton **a**, and two signals of pyridine β-protons **b**, arbitrarily assigned as **b1** and **b2**. The signal of proton **b1** is NOESY correlated to signals of a geminal pair of methylene protons **c1** and **d1**; similarly, the signal of proton **b2** is NOESY correlated to signals of protons **c2** and **d2**. The methylene signals are in turn COSY correlated to the respective signals of NH protons **e1** and **e2**, which in turn are correlated to signals of protons **f1** and **f2**, respectively. The analysis of the remaining COSY and NOESY/ROESY correlations within the cyclohexane ring allows assignment of the remaining signals (Figure 2). The HMQC spectrum in combination with the assignment of ^{1}H NMR signals also enable the assignment of ^{13}C NMR signals of the corresponding carbon atoms.

In the case of the $[EuL1](NO_3)_3$ complex (Figure 2), the integration of the spectrum easily shows the signals of intensity 1H, corresponding to the two γ-pyridine positions, one of them was arbitrarily assigned as **a1** and the other as **a2**. The rest of the signals were assigned in a similar fashion

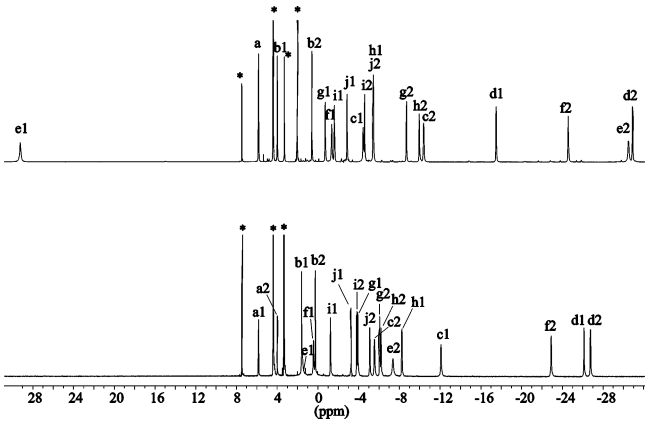

Figure 2. ^{1}H NMR spectra ($CD_3OD/CDCl_3$ 1:2 v/v solution, 298 K) of $[EuL]_2[Eu(NO_3)_5](NO_3)_4\cdot 3CH_3CN$ (upper trace) and $[EuL1](NO_3)_3\cdot CH_3OH\cdot H_2O$ (lower trace) complexes. Asterisks indicate residual solvents signals.

as described above for the complex of macrocycle L (Supporting Figures S2−S5). The assignment of NMR signals based on 2D NMR spectra was also done for the $[NdL](NO_3)_3$ complex (Supporting Figure S6).

It is interesting to compare the NMR spectra of $[EuL](NO_3)_3\cdot 3H_2O$ or $[EuL]_2[Eu(NO_3)_5](NO_3)_4\cdot 3CH_3CN$ complexes with the spectra of $[EuL1](NO_3)_3\cdot CH_3OH\cdot H_2O$ complex (Figure 2). The number of lines and the 2D NMR spectra reflect the symmetry of the complexes. The symmetry of $[EuL](NO_3)_3$ complex is C_2 and is reflected by the equal intensity of all 19 ^{1}H NMR signals and the presence of single γ-pyridine signal, which is COSY correlated to two β-pyridine protons. The symmetry of $[EuL1](NO_3)_3$ is C_s and is reflected by the presence of two pairs of coupled γ-pyridine and β-pyridine protons and the reduced intensity of two out of twenty ^{1}H NMR signals, corresponding to two different γ-pyridine positions. It should also be noted that the chemical shifts of the two complexes are very different, reflecting the sensitivity of NMR of paramagnetic macrocyclic complexes of lanthanide(III) ions to rather small variations of macrocyclic structure or axial ligation.[20−22]

The number of observed ^{1}H NMR resonances for $[LnL]^{3+}$ (19 signals) and $[LnL1]^{3+}$ (20 signals) complexes is much higher than that observed for the Ln(III) complexes of the parent Schiff base macrocycles (8 signals). In the latter case, the dynamic ligand exchange, accompanied by averaging of the macrocycle conformation, leads to higher effective symmetry in solution (D_2 and C_{2h} for the Schiff base analogues of the complexes of L and L1, respectively) than the symmetry observed in the solid state.[20,22] In the case of complexes of L and L1, this process may be much slower or does not take place. In fact, the X-ray crystal structures of these complexes (vide infra) suggest that even a fast ligand exchange will not lead to "averaging" of the two sides of the macrocycle.

X-ray Crystal Structures of the $[PrL(NO_3)(H_2O)_2](NO_3)_2$, $[EuL(NO_3)(H_2O)_2](NO_3)_2$, $[DyL(NO_3)_2]_2[Dy(NO_3)_5]\cdot 5CH_3CN$, $[YbL(NO_3)_2]_2[Yb(NO_3)_5]\cdot 5CH_3CN$, and $[EuL1(NO_3)(H_2O)_2]_{0.52}[EuL1(NO_3)_2]_{0.48}(NO_3)_{1.52}\cdot 0.48H_2O$ Complexes. The asymmetric unit of the $[EuL(NO_3)(H_2O)_2](NO_3)_2$ complex consists of two complex cations $[EuL(NO_3)(H_2O)_2]^{2+}$ and four nitrate anions. The two independent complex cations are very similar. In each complex cation, the Eu(III) ion adopts rather irregular geometry; the 10-coordinate Eu(III) ion is coordinated by six nitrogen atoms of the macrocycle L, bidentate nitrate anion, and two water molecules positioned on the opposite side of the macrocycle (Figure 3, Tables 1 and 2). The isomorphic $[PrL(NO_3)(H_2O)_2](NO_3)_2$ complex (Supporting Figure S7) is almost identical with that of Eu(III) complex, except the small differences in metal−ligand bond lengths related to larger size of Pr(III) (Table 2).

The asymmetric unit of the $[YbL(NO_3)_2]_2[Yb(NO_3)_5](NO_3)_4\cdot 5CH_3CN$ complex consists of two complex cations $[YbL(NO_3)_2]^+$, complex anion $[Yb(NO_3)_5]^{2-}$, and five acetonitrile solvate molecules. In each macrocyclic complex cation Yb(III) ion adopts irregular geometry; the 10-coordinate Yb(III) ion is coordinated by six nitrogen atoms of the macrocycle L and two axial bidentate nitrate anions bound on the opposite sides of the macrocycle (Figure 4). The structure of the $[DyL(NO_3)_2]_2[Dy(NO_3)_5]\cdot 5CH_3CN$ complex (Supporting Figure S8) is isomorphic with that of Yb(III) derivative.

The crystal of the $[EuL1(NO_3)(H_2O)_2]_{0.52}[EuL1(NO_3)_2]_{0.48}(NO_3)_{1.52}\cdot 0.48H_2O$ complex is highly disordered. It contains two different complex cations, $[EuL1(NO_3)(H_2O)_2]^{2+}$ and $[EuL1(NO_3)_2]^+$, randomly occupying the crystallographic sites with almost equal occupation (Figure 3). The 10-coordinate Eu(III) ion in $[EuL1(NO_3)(H_2O)_2]^{2+}$ complex cation has the same environment as in the above $[EuL(NO_3)(H_2O)_2]^{2+}$ complex, while the 10-coordinate Eu(III) in $[EuL1(NO_3)_2]^+$ complex has the same environment as Yb(III) ion in the above $[YbL(NO_3)_2]^+$ complex.

The lanthanide(III) ions seem to be slightly too small for most of the hexaazamacrocycle ligands. For this reason, these ligands adjust their conformation to match the size of the coordinated metal ion. This adjustment is based on combination of various degree of bending and helical twisting of the macrocycle.[1] In some cases, practically no bending is observed, and the helical twist determines the macrocycle conformation ("twist−wrap" conformation), as is observed in the nitrate Ln(III) complexes of the macrocyclic imine analogue of L.[23] In the $[LnL(NO_3)(H_2O)_2](NO_3)_2$ and $[LnL(NO_3)_2]_2[Ln(NO_3)_5]\cdot 5CH_3CN$ complexes, the macrocycle L adopts the most common "twist−fold" conformation; in these cases, the folding results in saddle-shaped ligand (Figure 4). While the angle between the two pyridine planes reflects both folding and twisting, the improper torsion angle C2−C4−C15−C17 reflects the twist of the two pyridine frag-

(20) (a) Lisowski, J.; Ripoli, S.; Di Bari, L. *Inorg. Chem*. **2004**, *43*, 1388−1394. (b) Lisowski, J. *Magn. Reson. Chem*. **1999**, *37*, 287−294. (c) Lisowski, J.; Mazurek, J. *Polyhedron*, **2002**, *21*, 811−816. (d) Lisowski, J.; Starynowicz, P. *Polyhedron* **1999**, *18*, 443−450.

(21) Lisowski, J.; Sessler, J. L.; Lynch, V.; Mody, T. D. *J. Am. Chem. Soc.* **1995**, *117*, 2273−2285.

(22) Gregoliński, J.; Kochel, A.; Lisowski, J. *Polyhedron* **2006**, *25*, 2745−2754.

(23) Lisowski, J.; Starynowicz, P. *Polyhedron* **2000**, *19*, 465−469.

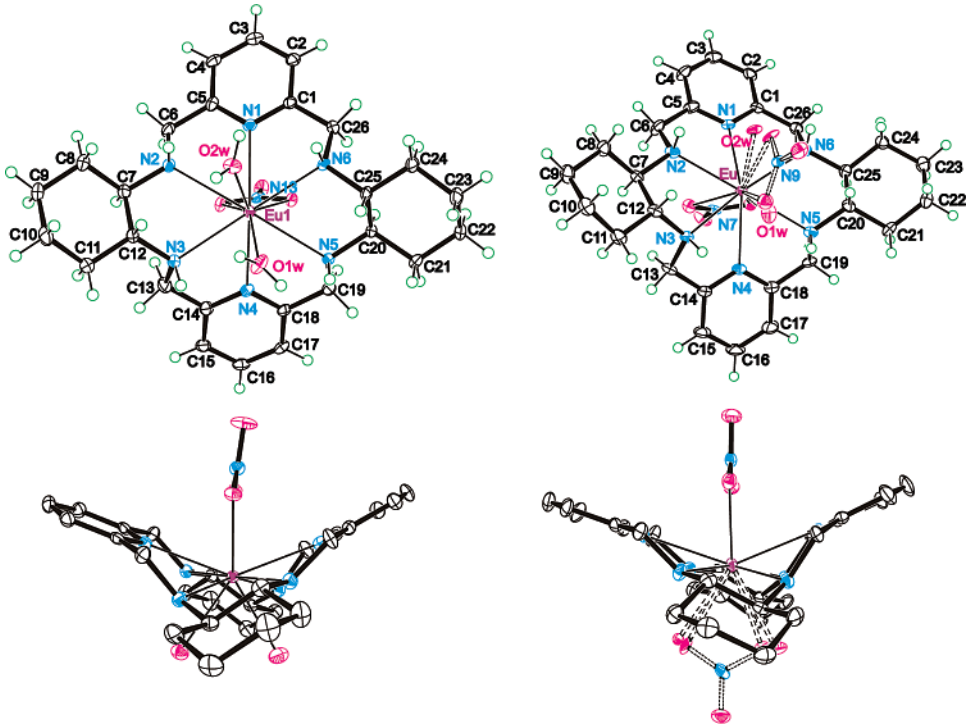

Figure 3. Top and side views of the complex cations of Eu(III) with the macrocycles L (left) and L1 (right). Dashed lines indicate disordered axial ligands.

Table 2. Bond Lenghs (Å) of the Complexes

$[LnL(NO_3)(H_2O)_2](NO_3)_2$

cation A	Ln = Pr	Ln = Eu	cation B	Ln = Pr	Ln = Eu
Ln(1)−N(1)	2.649(4)	2.604(3)	Ln(2)−N(7)	2.614(4)	2.582(3)
Ln(1)−N(2)	2.702(3)	2.680(3)	Ln(2)−N(8)	2.699(4)	2.676(3)
Ln(1)−N(3)	2.640(4)	2.610(3)	Ln(2)−N(9)	2.640(3)	2.604(2)
Ln(1)−N(4)	2.622(4)	2.592(3)	Ln(2)−N(10)	2.614(4)	2.570(3)
Ln(1)−N(5)	2.698(3)	2.664(3)	Ln(2)−N(11)	2.693(4)	2.665(3)
Ln(1)−N(6)	2.646(3)	2.597(3)	Ln(2)−N(12)	2.644(3)	2.607(3)
Ln(1)−O(13*B*)	2.569(3)	2.514(2)	Ln(2)−O(14*B*)	2.605(3)	2.551(2)
Ln(1)−O(13*C*)	2.608(3)	2.552(2)	Ln(2)−O(14*C*)	2.579(4)	2.507(3)
Ln(1)−O(1*W*)	2.549(3)	2.486(2)	Ln(2)−O(3*W*)	2.646(3)	2.613(3)
Ln(1)−O(2*W*)	2.556(3)	2.511(2)	Ln(2)−O(4*W*)	2.526(3)	2.481(3)

$[LnL(NO_3)_2]_2[Ln(NO_3)_5]\cdot 5CH_3CN$

cation A	Ln = Dy	Ln = Yb	cation B	Ln = Dy	Ln = Yb
Ln(1)−N(1)	2.517(5)	2.490(5)	Ln(2)−N(7)	2.539(5)	2.502(5)
Ln(1)−N(2)	2.604(5)	2.597(5)	Ln(2)−N(8)	2.591(5)	2.568(5)
Ln(1)−N(3)	2.535(5)	2.504(5)	Ln(2)−N(9)	2.550(5)	2.533(5)
Ln(1)−N(4)	2.507(6)	2.476(5)	Ln(2)−N(10)	2.541(6)	2.516(5)
Ln(1)−N(5)	2.612(5)	2.591(5)	Ln(2)−N(11)	2.601(5)	2.583(5)
Ln(1)−N(6)	2.537(5)	2.498(5)	Ln(2)−N(12)	2.561(5)	2.534(5)
Ln(1)−O(13*B*)	2.502(5)	2.448(5)	Ln(2)−O(15*B*)	2.497(5)	2.454(4)
Ln(1)−O(13*C*)	2.502(5)	2.456(5)	Ln(2)−O(15*C*)	2.477(5)	2.439(4)
Ln(1)−O(14*B*)	2.515(4)	2.484(4)	Ln(2)−O(16*B*)	2.506(4)	2.472(4)
Ln(1)−O(14*C*)	2.516(5)	2.481(4)	Ln(2)−O(16*C*)	2.558(4)	2.536(4)

$[YbL(H_2O)_2](NO_3)_3\cdot H_2O$

Yb(1)−N(1)	2.400(2)	Yb(1)−N(4)	2.420(2)	Yb(1)−O(1*W*)	2.302(2)
Yb(1)−N(2)	2.480(2)	Yb(1)−N(5)	2.452(2)	Yb(1)−O(2*W*)	2.317(2)
Yb(1)−N(3)	2.456(2)	Yb(1)−N(6)	2.451(2)		

$[EuL1(NO_3)(H_2O)_2]_{0.52}[EuL1(NO_3)_2]_{0.48}(NO_3)_{1.52}\cdot 0.48H_2O$

Eu(1)−N(1)	2.577(2)	Eu(1)−N(5)	2.614(3)	Eu(1)−O(9*B*)	2.53(2)
Eu(1)−N(2)	2.602(3)	Eu(1)−N(6)	2.619(2)	Eu(1)−O(9*C*)	2.60(1)
Eu(1)−N(3)	2.659(2)	Eu(1)−O(7*B*)	2.510(2)	Eu(1)−O(1*W*)	2.53(1)
Eu(1)−N(4)	2.603(3)	Eu(1)−O(7*C*)	2.497(2)	Eu(1)−O(2*W*)	2.60(2)

ments, and the angle determined by the two pyridine nitrogen atoms and the central metal ion reflects mainly the bending of the macrocycle. Similarly, the improper torsion angle C7−C12−C20−C25 reflects the twist of the two cyclohexane fragments. The improper torsion angle C2−C4−C15−C17 is equal to −13.3(2), −10.8(2), −13.3(3), and −4.1(3)° for the two independent complex cations of $[EuL(NO_3)(H_2O)_2](NO_3)_2$ and the two independent complex cations of $[YbL(NO_3)_2]_2[Yb(NO_3)_5]\cdot 5CH_3CN$, respectively, reflecting only moderate helical twist. The N1−Ln(III)−N4 angle for these four complex cations is equal to 139.1(1), 138.0(1), 140.2(2), and 140.3(2)°, respectively. Similar values (−11.0(2), −10.2(2), −13.5(3), and −4.3(3)°) of the C2−C4−C15−C17 improper torsion angle are observed for the Pr(III) complex isomorphic with $[EuL(NO_3)(H_2O)_2](NO_3)_2$ and the Dy(III) complex isomorphic with $[YbL(NO_3)_2]_2[Yb(NO_3)_5]\cdot 5CH_3CN$.

The X-ray crystal structures discussed above confirm the C_2 symmetry of the L complexes and the C_s symmetry of the L1 complexes observed by NMR spectroscopy. They reveal also an important feature: all the amine protons, NH, point to one side of the macrocycle (corresponding to SRSR configuration at the amine nitrogen atoms for Eu(III) complexes of both L and L1, Figure 3). In such a conformation, the two sides of the macrocycle will not become effectively equivalent in the NMR time scale even when a fast ligand exchange and bending of the macrocycle take place. For this reason, the higher effective D_2 symmetry observed in the case of Ln(III) complexes of the imine analogue of L,[20c] related to observation of lower number of ^{1}H NMR signals, is not possible for the complexes of L. For similar reasons, the effective higher C_{2h} symmetry observed for Ln(III) complexes of the imine analogue of L1[22] is not possible for complexes of L1.

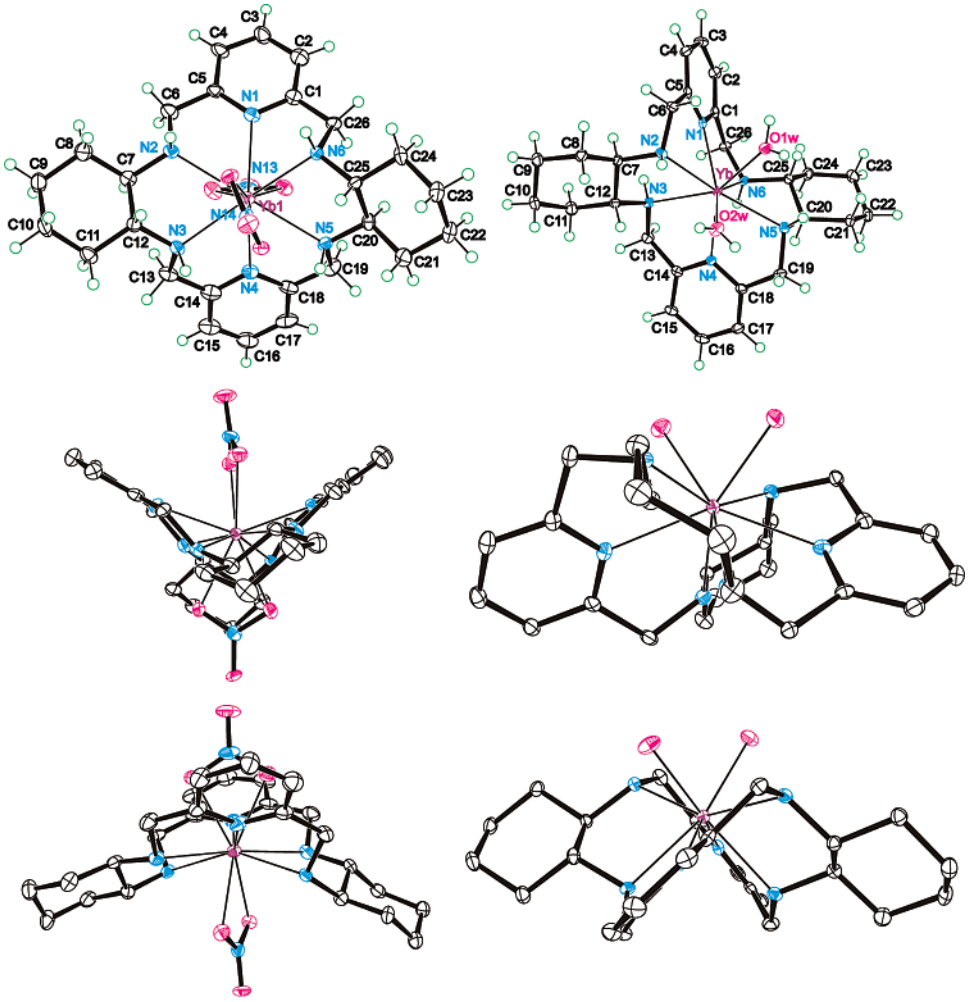

Figure 4. Top and side views (roughly along the cyclohexane rings and roughly along the pyridine rings) of the $[YbL(NO_3)_2]^+$ (left, SRSR configuration at the amine N atoms) and $[YbL(H_2O)_2]^{3+}$ (right, SSSS configuration at the amine N atoms) complex cations.

In the case of the Eu(III) complex of macrocycle L1, the RR and SS configuration of the stereogenic carbon atoms of the two diaminocyclohexane rings imposes C_s symmetry of the macrocycle. For this reason, the cationic complexes in $[EuL1(NO_3)(H_2O)_2]_{0.52}[EuL1(NO_3)_2]_{0.48}(NO_3)_{1.52}\cdot 0.48H_2O$ exhibit practically no helical twist. The improper torsion angle C2−C4−C15−C17 is equal to 0.1(2)°, and the N1−Eu−N4 angle reflecting the fold of the macrocycle is equal to 138.7(1)°. The overall shape of L and L1 macrocycles in their Eu(III) complexes is very similar; the main difference is the mutual orientation of the cyclohexane fragments (Figure 3). In the case of the complex with the *meso*-macrocycle L1, the value of improper torsion angle C7−C12−C20−C25 is close to zero (2.9(2)°), reflecting the approximate C_s symmetry, while in the complex of the macrocycle L, this value is equal to 78.6(3) and 71.4(2)° for the two independent cationic complex molecules, reflecting the chiral nature of the macrocycle L.

The conformation of the macrocycle L in the discussed Pr(III), Eu(III), Dy(III), and Yb(III) complexes is very similar to that observed in the previously reported La(III) complex[5] (improper torsion angle C2−C4−C15−C17 equal to −18.6° for the (RRRR) isomer and the N1−La(III)−N4 angle equals 146.3°). The larger La(III) ion is 11-coordinate and is coordinated by two bidentate and one monodentate nitrate anions. Moreover, the complex is of lower (C_1) symmetry because of the irregular configuration at the stereogenic amine nitrogen atoms (RRRS configuration at nitrogen atoms for the enantiomer corresponding to the (RRRR) configuration at the carbon atoms).

Helicity Inversion in $[YbL]^{3+}$ and the X-ray Crystal Structure of $[YbL(H_2O)_2](NO_3)_3\cdot H_2O$. The $[YbL]_2[Yb(NO_3)_5](NO_3)_4\cdot 2H_2O$ complex, synthesized in organic solvent, after dissolution in water undergoes a slow change into new complex form, as revealed by ^{1}H NMR and CD spectra (Figure 5, Supporting Figure S9). The ^{1}H NMR spectrum of the new form of the Yb(III) complex corresponds to the spectrum of the isolated pure $[YbL(H_2O)_2](NO_3)_3$ complex synthesized in water. The mixtures of the above two forms of the Yb(III) complex were also observed in some unsuccessful preparations of the Yb(III) complex.

In the case of the Ln(III) complexes of the Schiff base analogue of L, the new form of complexes appearing in D_2O solution corresponds to hydroxo species arising from slow hydrolysis of the starting complexes.[4,24] To verify the

(24) Lisowski, J.; Starynowicz, P. *Inorg. Chem. Comm.* **2003**, *6*, 593−597.

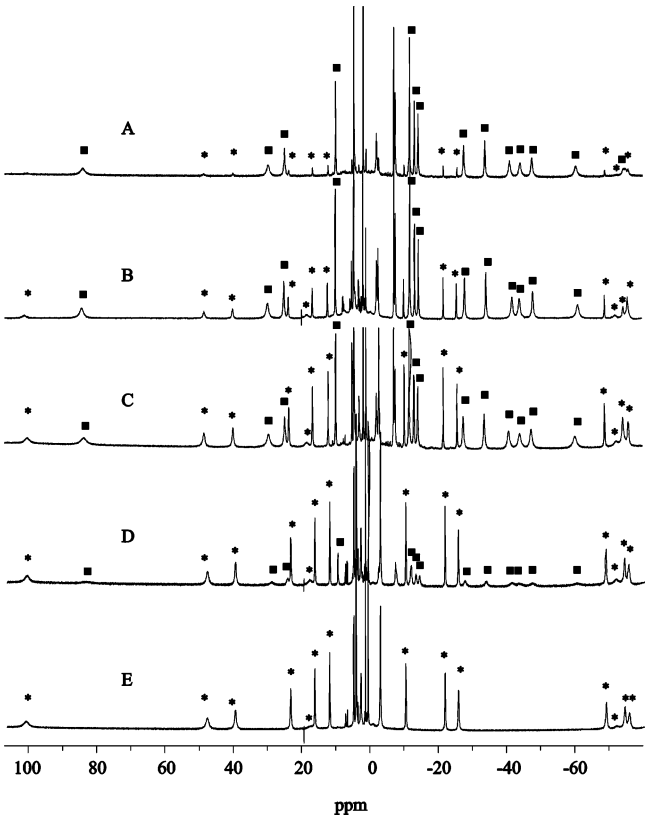

Figure 5. Conversion of the $[YbL^2]_2[Yb(NO_3)_5](NO_3)_4 \cdot 2H_2O$ complex in D_2O (7 mM solution). The ^1H NMR spectra (298K) were recorded 10 min (A), 3 h (B), 24 h (C), 48 h (D), and 72 h (E) after dissolution of the complex. Squares denote the signals of the starting isomer of the complex, and the asterisks denote the new isomer.

possibility of formation of similar hydroxo complexes, the NMR titrations of both $[YbL]_2[Yb(NO_3)_5](NO_3)_4 \cdot 2H_2O$ and $[YbL(H_2O)_2](NO_3)_3$ complexes with solution of NaOH were performed. In these titrations, the macrocyclic hydroxo Yb(III) complexes are indeed formed, but this process does not correspond to the formation of the new form described above. After the addition of 0.5−2 equiv of NaOH in D_2O, broad poorly defined spectra are obtained (indicating exchange process of intermediate rate on the NMR time scale), but these spectra are different for the $[YbL]_2[Yb(NO_3)_5](NO_3)_4 \cdot 2H_2O$ and $[YbL(H_2O)_2](NO_3)_3$ starting complexes. After addition of three or more equivalents of NaOH to the $[YbL(H_2O)_2](NO_3)_3$ complex, the spectrum of the final hydroxo complex is obtained, consisting of 34 well-resolved lines (Supporting Figure S10). This complex is most ikely a μ-dihydroxo dinculear complex analogous to dinuclear Ln(III) complexes with macrocylic hexaaza[4,24] or pentaaza[25] Schiff bases. The number of lines corresponds to 34 nonexchangeable signals of macrocycle L in a complex of C_1 symmetry.

The origin of the difference between the two forms of the Yb(III) complex is revealed by the X-ray crystal structure (Figure 4) of the complex crystallized from the aqueous solution of $[YbL(H_2O)_2](NO_3)_3$. The asymmetric unit of the obtained $[YbL(H_2O)_2](NO_3)_3 \cdot H_2O$ crystals consists of complex cation $[YbL(H_2O)_2]^{3+}$, three nitrate anions, and the solvate water molecule. The 8-coordinate Yb(III) ion is coordinated by the six nitrogen atoms of the macrocycle L and two axial water molecules positioned at the same side of the macrocycle. The coordination sphere around Yb(III) is highly distorted.

The difference in coordination number (8 vs 10) between the complexes $[YbL(H_2O)_2](NO_3)_3 \cdot H_2O$ and $[YbL(NO_3)_2]_2[Yb(NO_3)_5](NO_3)_4 \cdot 5CH_3CN$ does not directly explain the observation of two stable forms of Yb(III) complex in solution because, for the fluxional Ln(III) complexes, the coordination number may be different for the species observed in the solid state and in solution, and easy axial ligand exchange in solution is expected. More important differences between the structures of these two complexes complexes are the different configurations at the stereogenic amine nitrogen atoms and the different sense of helical twist of the macrocycle. As mentioned above, in the $[YbL(NO_3)_2]_2[Yb(NO_3)_5](NO_3)_4 \cdot 5CH_3CN$ complex, all the amine protons NH point to one side of the macrocycle, corresponding to the SRSR configuration at nitrogen atoms (thus to the RSRS configuration of the respective form of the free ligand L, Scheme. 1). In the $[YbL(H_2O)_2](NO_3)_3 \cdot H_2O$ complex, the NH protons point alternately above and below the macrocycle plane, corresponding to the SSSS configuration at amine nitrogen atoms (thus to the RRRR configuration of the respective form of the free ligand L, Scheme. 1). Yet another configuration at the nitrogen atoms (RRRS) is observed in the previously reported La(III) complex of the racemic macrocycle L.[5] To the best of our knowledge, this kind of stereoisomerism is demonstrated for the first time for the hexaazamacrocyclic complexes, while it is well-known for the tetraazamacrocyclic complexes.[7]

The different configuration at the amine nitrogen atoms in the two isomers is accompanied by the opposite sense of helical twist. The macrocycle L in $[YbL(H_2O)_2]^{3+}$ is folded in a manner similar to that in the other above-discussed complexes of L; the N1−Yb−N4 angle is equal to 136.9(1)°. In contrast, the helical twist of the macrocycle is much higher; the improper torsion angle C2−C4−C15−C17 is equal to 87.2(2)° in comparison with the −13.3(3)° and −4.1(3)° values observed for the $[YbL(NO_3)_2]^+$ complex cations. The extent of helical twist is unusually high for the hexaazamacrocyclic complex of lanthanide(III), while similar or even greater twist is observed for the complexes of transition metal ions.[5,26] Importantly, the sign of the angle is reversed, which corresponds to the opposite sense of helical twist and the presence of two diastereomeric macrocyclic units Λ-$[YbL]^{3+}$ and Δ-$[YbL]^{3+}$. This opposite direction of helical twist is also reflected by the mutual orientation of the cyclohexane fragments; the improper torsion angle C7−C12−C20−C25 is equal to −58.8(2)° for the $[YbL(H_2O)_2](NO_3)_3 \cdot H_2O$ complex, while this angle is equal to 72.8(5) and 67.1(4)° for the two independent complex molecules of $[YbL(NO_3)_2]_2[Yb(NO_3)_5] \cdot 5CH_3CN$. The opposite helical

(25) Patroniak, V.; Kubicki, M.; Mondry, A.; Lisowski, J. Radecka-Paryzek, W. *Dalton Trans.* **2004**, 3295−3304.

(26) (a) Bryant, L. H., Jr.; Lachgar, A.; Jackels, S. C. *Inorg. Chem.* **1995**, *34*, 4230−4238. (b) Bryant, L. H., Jr.; Lachgar, A.; Coates, K. S.; Jackels, S. C. *Inorg. Chem.* **1994**, *33*, 2219−2226.

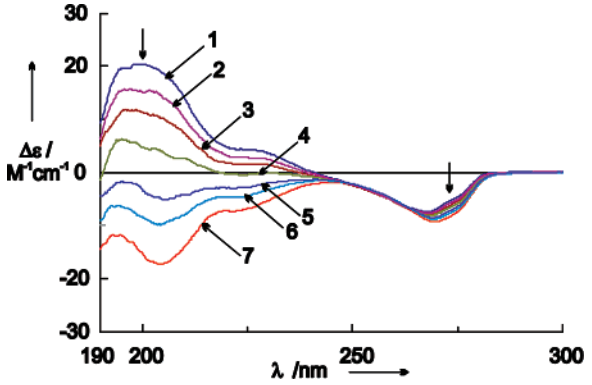

Figure 6. Conversion of the $[YbL(H_2O)_2](NO_3)_3$ complex in acetonitrile (0.27 mM solution); CD spectra measuread immediately after dissolution of the complex (1), after 0.5 h (2), after 1 h (3), after 2 h (4), after 4 h (5), after 6 h (6), and after 144 h (7).

Scheme 2. Proposed Mechanism of Helicity Inversion of the (RRRR)(RSRS) and (RRRR)(SSSS) Isomers of the Macrocycle L in Its Yb(III) Complexes

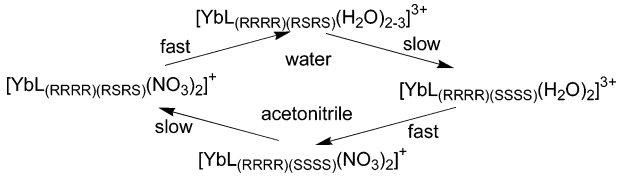

sense of the two isomers of the Yb(III) complex is manifested in very different CD spectra of the two isomeric Yb(III) complexes both in acetonitrile (Figure 6, Supporting Figure S11) and water (Supporting Figures S9, S11) solutions.

As mentioned above, the ^{1}H NMR spectra show that the (RRRR)(SRSR) isomer (corresponding to the X-ray crystal structure of $[YbL(NO_3)_2]^+$) is quantitatively converting to the (RRRR)(SSSS) isomer (corresponding to the X-ray crystal structure of $[YbL(H_2O)_2]^{3+}$) in water solution (Figure 5). This process is also visible in the CD spectra, although no clear isosbestic points are observed (Supporting Figure S9). The opposite process is observed for the acetonitrile solution (Figure 6, Supporting Figure S12). The CD and NMR spectra of both $[YbL]_2[Yb(NO_3)_5](NO_3)_4 \cdot 2H_2O$ and $[YbL(H_2O)_2](NO_3)_3$ are different for water and acetonitrile solutions. What is important, however, is that the final ^{1}H NMR spectrum obtained in the conversion of the $[YbL]_2[Yb(NO_3)_5](NO_3)_4 \cdot 2H_2O$ complex in D_2O (Figure 5) is identical to the spectrum of single crystals of $[YbL(H_2O)_2](NO_3)_3 \cdot H_2O$ dissolved in the same solvent (Supporting Figure S13). Similarly, the ^{1}H NMR spectrum of the final form obtained in the conversion of the $[YbL(H_2O)_2](NO_3)_3$ complex in CD_3CN (Supporting Figure S12) is identical to the spectrum of single crystals of $[YbL]_2[Yb(NO_3)_5](NO_3)_4 \cdot 2H_2O$ dissolved in the same solvent.

The different stability of the isomers of the Yb(III) complex in water and acetonitrile solutions probably reflects the kind of axial ligands preferred in these two solvents. Likely the nitrate and solvent axial ligands can be easily replaced, followed by the reorganization of the macrocycle, as presented in Scheme 2. The overall conformation of macrocycle L is very different in the two isomers; in general, the ligand L is somewhat more "squeezed" in the (RRRR)-(SSSS) isomer and more "open" in the (RRRR)(SRSR) isomer (Figure 4, Supporting Figure S14). The bulkier nitrate axial ligands and the 10-coordinate Yb(III) ions are more compatible with the more open form of the macrocycle, while the smaller water axial ligands and the 8-coordinate Yb(III) ion are more compatible with the more squeezed form of L. In water solution, the axial sites are occupied by water molecules, while in the less polar organic solvents, the more bulky nitrate anions are bound in axial positions. Thus the different kind of the preferred isomer in water and acetonitrile solutions reflects the steric requirements of the axial ligands and the stabilization of the more charged complex in water solution.

The changes in time of the CD spectrum of a water solution of Dy(III) (and to some extent of Eu(III)) complex with L are similar to those observed for the Yb(III) complex, suggesting the same helicity inversion process. In the case of these complexes, however, the ^{1}H NMR spectra of D_2O solutions are severely broadened by chemical exchange (most likely corresponding to axial ligand exchange), and single crystals of the second isomer have not been obtained.

Solvent effects on chirality and helicity inversion[9−11] are topics of considerable interest. Described here, the quantitative conversion of the (RRRR)(SRSR) isomer into (RRRR)-(SSSS) isomer of Yb(III) complex in water solution and the opposite conversion in acetonitrile solution represent a very rare case of control of helicity inversion in well-defined chemical compounds by the choice of the solvent. Solvent-induced helicity inversion in metal complexes[9c] or organic polymeric systems[10a,b] most often results from switching of intramolecular hydrogen bonding. However, in the case of octahedral Co(II) complexes with the chiral tetradendate ligand, the helicity inversion is based on the exchange of anion for solvent molecules in the coordination sphere of the metal ion.[9a,b] In these Co(II) complexes, the ligand is more flexible, so both the solvent−anion exchange and reorganization of the ligand are fast processes, leading to a simpler mechanism of helicity inversion in comparison with that presented in Scheme 2.

Conclusions

The macrocyclic hexaaza tetraamine macrocycle L forms a number of enantiopure complexes with lanthanide(III) ions, differing in composition and axial ligation. The 2D NMR spectra of Ln(III) complexes with the chiral macrocycle L and its *meso*-type isomer L1 are consistent with the X-ray crystal structures and indicate the C_2 and C_s symmetry of these complexes, respectively. In the case of Yb(III) complex with L, two forms, $[YbL(NO_3)_2]^+$ and $[YbL(H_2O)_2]^{3+}$, which differ in the direction of helical twist and the configuration at the stereogenic amine nitrogen atoms, have been selectively obtained. It should be noted that the two forms of the macrocycle L observed in the $[YbL(NO_3)_2]^+$ and $[YbL(H_2O)_2]^{3+}$ complexes are not merely two different conformations, but two genuine diastereomers of this macrocycle related to hampered NH exchange caused by complexation of metal ion. The two isomeric forms may be selectively

interconverted in water and acetonitrile, in this way representing the helicity inversion process controlled by the solvent.

Acknowledgment. This work was supported by MNiSW Grant 1 T09A 143 30.

Supporting Information Available: Figures S1−S14 (ESI MS, 2D NMR, ^{1}H NMR, and CD spectra, views of molecular structures) and X-ray crystallographic information in CIF format. This material is available free of charge via the Internet at http://pubs.acs.org.

IC700831Z